美国摄影光学仪器工程师学会—国际光学工程学会会议录
第439卷：微微秒光电子学

PROCEEDINGS

Of SPIE-The International Society for Optical Engineering

Volume 439

Picosecond Optoelectronics

Gerard Mourou
Chairman/Editor

August 24-26, 1983
San Diego, California

Proceedings of SPIE—The International Society for Optical Engineering

Volume 439

Picosecond Optoelectronics

Gerard Mourou
Chairman/Editor

August 24–26, 1983
San Diego, California

Published by
SPIE—The International Society for Optical Engineering
P.O. Box 10, Bellingham, Washington 98227-0010 USA
Telephone 206/676-3290 (Pacific Time) • Telex 46-7053

The papers appearing in this book comprise the proceedings of the meeting mentioned on the cover and title page. They reflect the authors' opinions and are published as presented and without change, in the interests of timely dissemination. Their inclusion in this publication does not necessarily constitute endorsement by the editors or by SPIE.

Please use the following format to cite material from this book:
Author(s), "Title of Paper," *Picosecond Optoelectronics,* Gerard Mourou, Editor, Proc. SPIE 439, page numbers (1983).

Library of Congress Catalog Card No. 83-051015
ISBN 0-89252 474-X

Printed in the United States of America.

PICOSECOND OPTOELECTRONICS

Volume 439

Conference Committee

Chairman
Gerard Mourou
University of Rochester

Co-Chairmen
David M. Bloom
Hewlett-Packard Laboratories

Michael A. Duguay
Bell Laboratories/Holmdel

Chi H. Lee
University of Maryland

Fred J. Leonberger
Massachusetts Institute of Technology, Lincoln Laboratory

P. T. Ho
University of Maryland

Session Chairman
Session 1—Picosecond Phenomena in Semiconductors
Michael A. Duguay, Bell Laboratories/Holmdel

Session 2—Semiconductor Lasers
P. T. Ho, University of Maryland

Session 3—Picosecond Photoconductive Switching and Applications
Gerard Mourou, University of Rochester

Session 4—Electrical Signal Sampling and Signal Processing
David M. Bloom, Hewlett-Packard Laboratories

Session 5—Fast Photodetectors
Fred J. Leonberger, Massachusetts Institute of Technology, Lincoln Laboratory

PICOSECOND OPTOELECTRONICS

Volume 439

INTRODUCTION

Due to the recent advances in laser techniques and materials, several areas in the field of optoelectronics have exhibited a rapid growth. This rapid expansion has been driven by the need for faster electronics, computers and communications. The object of this conference was to bring together scientists from the different disciplines of optoelectronics working in the picosecond time-scale.

The meeting was divided into four sessions highlighting recent advances in material and device development and understanding. The first session was devoted to the interaction of light and semiconductors where theoretical and experimental works on carrier kinetics and nonlinear transport in semiconducting material were presented. This session was followed by recent advances in short pulse generation with laser diodes. Passively and actively mode locked systems were described as well as work on laser diodes modulated in the x-band regime. The next two sessions dealt with the new field of picosecond photoconductive switching and its applications in low and high power regimes. Work on picosecond and subpicosecond electrical pulse generation and characterization were discussed. On the high power side, new semiconductive materials and switch designs were introduced. The meeting was concluded with a discussion of recent work on fast detectors. Devices with picosecond resolution and sensitivity enhancement techniques were highlighted.

This volume represents the proceedings of this conference on picosecond optoelectronics, where thirty-six papers were presented. The conference was organized and chaired by G. Mourou from the University of Rochester, M. Duguay and P. Downey from Bell Laboratories, D. M. Bloom from Hewlett-Packard, C. H. Lee and P. T. Ho from the University of Maryland, and F. J. Leonberger from MIT/Lincoln Laboratory.

Gerard Mourou
University of Rochester

PICOSECOND OPTOELECTRONICS

Volume 439

Contents

PICOSECOND OPTOELECTRONICS

Volume 439

Session 1

Picosecond Phenomena in Semiconductors

Chairman
Michael A. Duguay
Bell Laboratories/Holmdel

Femtosecond optical pulses and technology

R. Yen, C. V. Shank, and R. L. Fork

Bell Telephone Laboratories
Holmdel, New Jersey 07733

Abstract

In this discussion, we report two recent advances in femtosecond optical technology. Firstly, the generation and measurement of optical pulses as short as 30 fs is described. The pulses are produced using self-phase modulation of the 90 fs laser pulse in a short 15 cm optical fiber followed by a grating compressor.

Finally, we report the operation of an optically synchronized streak camera which operates at 10 Hz repetition rate and has a system jitter of less than one picosecond. Synchronization is achieved with a Fe:InP photoconductive switch which allows for room temperature dc biasing.

Introduction

Considerable progress has taken place in the last decade and a half in the generation of ultrashort optical pulses. The first key advance was the improvement of the passively modelocked dye laser using the colliding pulse modelocked dye laser configuration.[1] With this (CPM) laser the first pulses with a duration of less than 90 femtosecond were generated. The second important result is an improvement in amplification technique which has permitted the generation of femtosecond optical pulses of gigawatt intensities.[2] In this discussion, we report two more recent advances in femtosecond optical technology. Firstly, the generation and measurement of optical pulses as short as 30 fs is described.[3] Lastly, we report the operation of an optically synchronized streak camera with a system jitter of less than one picosecond.[4]

30 Femtosecond optical pulses

In this section we report the generation and measurement of an optical pulse only 30 femtoseconds (3×10^{-14}sec) in duration using optical compression techniques. This is the shortest optical pulse ever generated using laser techniques and corresponds to 14 optical cycles. We produce these extremely short pulses by using nonlinear frequency broadening in a short piece of optical fiber followed by compression with a dispersive delay line.[3] Previous authors have anticipated the possibility of compressing extremely short optical pulses.[5] In this communication we will describe an extension of these pulse compression techniques to the femtosecond time regime.

The experimental arrangement for pulse compression is shown in Figure 1. Optical pulses, of duration 90 fsec at a wavelength of 619 nm obtained from a modelocked colliding pulse ring dye laser,[1] are amplified with a four stage dye amplifier[2] pumped by a frequency doubled Nd:YAG laser. The amplified pulse also has a duration of 90 fs. The amplified pulse is then attenuated to a predetermined level and is focused into a 15 cm long single-mode polarization preserving optical fiber. For a few nJ energy coupled into the optical fiber the optical spectrum is observed to broaden significantly. With increasing input energy the spectrum continues to broaden until a white light continuum covering nearly the entire optical spectrum is generated. The light from the fiber was recollimated with a lens and passed through a grating compressor.[3]

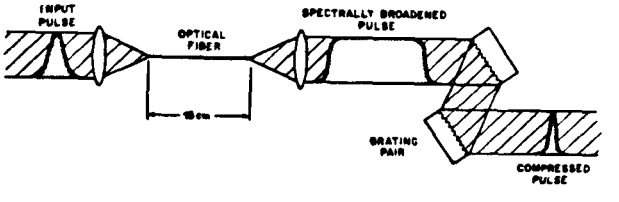

Figure 1. Diagram of experiment.

We have chosen the second harmonic autocorrelation method to measure the optical pulse. This technique has been used successfully to measure optical pulses in the picosecond range. As optical pulsewidths approach the femtosecond time regime possible sources of error must

be considered. The first requirement is that the entire optical spectrum of the pulse must be upconverted. This can be assured by broadening the phasematching condition using a sufficiently thin crystal and generating the second harmonic at the focus of a lens. The second important point is to consider the influence of group velocity dispersion.

The optical elements used to recollimate the beam exiting from the fiber and to direct the pulses into the second harmonic crystal all contribute to the group velocity dispersion experienced by the pulse. Fortunately, the grating compressor used in the experiment compresses the chirped pulse and provides a means of compensating other dispersive elements in the beam as well.

The optical energy coupled into the optical fiber was adjusted to produce about a factor of three increase in the frequency spectrum. The spectral halfwidth broadened from about 60Å to about 200Å halfwidth. This spectral width approached the phasematching bandwidth of our measurement crystal. We used a grating pair with 600 lines/mm and slant angle of 30° set 6.4 cm apart to obtain optimum pulse compression. The result shown in Figure 2 is the autocorrelation of an optimally compressed pulse. Note that the pulse is very clean with very little energy in the wings. The measured halfwidth of the autocorrelation function is 45 fsec corresponding to an optical pulse of approximately 30 fsec.

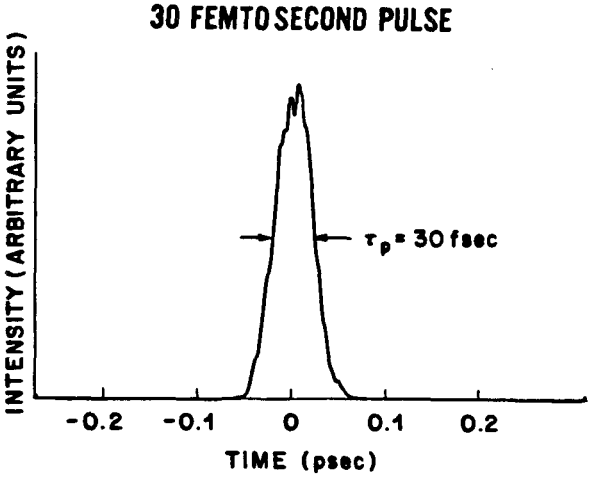

Figure 2. Pulsewidth autocorrelation using the phasematched second harmonic technique in a .2 mm KDP crystal. The autocorrelation halfwidth is 45 fsec corresponding to a 30 fsec optical pulsewidth.

Subpicosecond jitter streak camera

The dynamic range of a streak camera can be greatly increased when data can be accumulated from several laser pulse initiated events. The principle problem is that triggering jitter resulting from imprecise synchronization of the streak camera and the laser pulse tends to reduce the temporal resolution of the camera. Recently two groups, Margulis, et.al.[6] and Mourou, et.al.[7] have utilized a laser triggered photoconductive switch to synchronize a streak camera to a short laser pulse. Mourou, et.al. using 30 picosecond pulses were able to determine that the system drift was less than 2 picoseconds, but unfortunately were unable to time resolve the synchronized camera time response with such long laser pulses. In this paper we describe the first operation of a synchronized streak camera operating at 10 Hz with system pulse to pulse jitter determined to be less than 1.0 picosecond using 90 femtosecond optical pulses.

Figure 3 is a schematic diagram of our system. The streak tube (enclosed in dotted lines) is an ITT visible proximity focused streak tube consisting of the photocathode (a), the collimating microchannel plate (b), the deflection plates (c) and the phosphor screen (d). The streak tube output image is coupled by the reducing fiber optics bundle (e) onto the ITT image intensifier (f), the output of which is fiber optics coupled onto the Princeton Applied Research silicon intensifier tube (h), whose output is then displayed on the OMA monitor screen. All optical surfaces are in direct contact and are index matched with the Optical Couplant manufactured by 3M.

The deflection plates of the streak tube are externally connected via flexible copper strips to the 100 pf storage capacitor. The photoconductive switch that completes the circuit is a 1 cm x 1 cm x 0.05 cm piece of iron doped InP.[8] This semi-insulating InP material is chosen to minimize thermal run away hence allowing for room temperature and high

voltage dc biasing of the switch. The 5 mm gap on our switch can hold off about 14 kV. Gold contacts are evaporated onto the InP and make electrical contact with the copper strip lines via the silver paint.

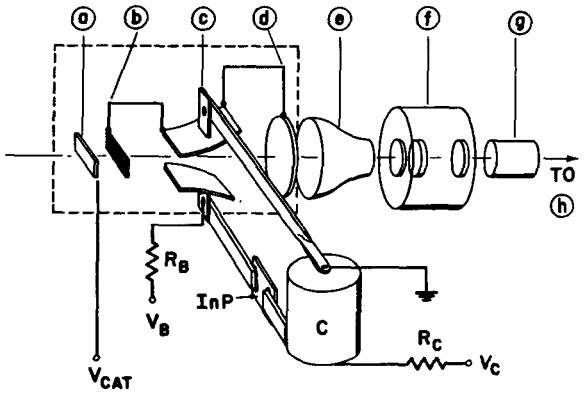

Figure 3. Schematic diagram of the streak camera: (a) photocathode, (b) microchannel collimator, (c) deflection electrodes, (d) phosphor screen, (e) reducing fiber optics coupler, (f) image intensifier, (g) fiber optics coupler, (h) silicon intensified target tube and OMA monitor; C is the 100 pf storage capacitor, the biasing resistor R_B=25 Mohm and the charging resistor R_C=22 Mohm.

During operation of the camera, a negative 8kV is applied to the photocathode (V_{cat}). The dc bias voltage V_B on the lower sweep plate is set at -1 kV to deflect any ambient light induced photocurrent off the phosphor screen. A positive voltage V_C is applied across the storage capacitor resulting in a total voltage of $V_O=V_C+V_B$ applied across the InP switch. Under continuous 10 Hz triggering, the 5 mm gap switch at room temperature limits V_O to about 14 kV.

The 90 femtosecond laser pulses used in the testing of this camera are generated by the colliding pulse mode-lock oscillator[1] and are subsequently amplified by a 10 Hz amplifier chain.[2] Part of these laser pulses are split off to trigger the InP switch whereas the rest are sent through a variable delay line and are line focused onto the photocathode through a slit and lens system to a 100μm wide line which is chosen to correspond to the spatial resolution limit of the ITT streak tube.

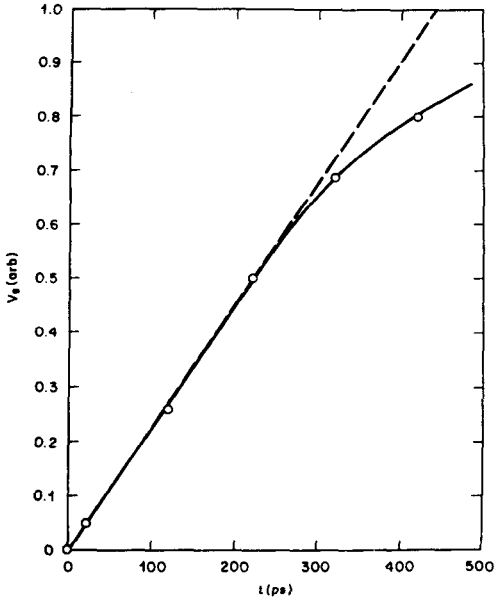

Figure 4. Voltage sweep across the streak tube after triggering of the InP switch. Data show the initial linear voltage ramp.

Figure 4 shows the initial voltage sweep across the streak tube after triggering of the InP switch. The rapid voltage sweep shows the charging of the 1 ps capacitance of the streak tube sweep electrodes by the 100 pf storage capacitor through the finite contact resistance and the finite resistance of the on-state InP switch. The initial linear voltage ramp is used as the operating range of the camera. As can be expected, voltage ringing is observed at later times. This can be eliminated by adding a damping resistor between the lower sweep electrode and the InP switch at the expense of reduced sweep rate.

Trade (a) in Figure 5 shows the 3.15 ps static resolution of our camera system as recorded on the OMA monitor. Trace (b) shows the single shot dynamic resolution of 3.8 ps achieved with V = 14 kV under saturation intensity on the switch. The practically jitter free operation of the system is realized when it is noted that trace (c) is actually a stacking of a sequence of 100 single events. The remaining jitter is due to the 10% energy fluctuation in the trigger laser pulses.

In conclusion, we demonstrated the real time monitoring of 10 Hz event using "single-shot" streak camera with subpicosecond jitter. In addition to the trigger timing jitter reduction resulted from the use of photoconductive switching,[6,7] the dc biasing of the Fe:InP switch[8] eliminated any possible voltage amplitude fluctuation induced streak rate variation inherent in any pulsed biasing scheme. The use of trigger laser pulses much shorter in duration than the single shot resolution limit of the camera system accounts for a further reduction in the shot-to-shot timing jitter. Finally, any remaining jitter due to trigger laser pulse amplitude fluctuation can be minimized by operating at the conductance saturation regime of the switch.

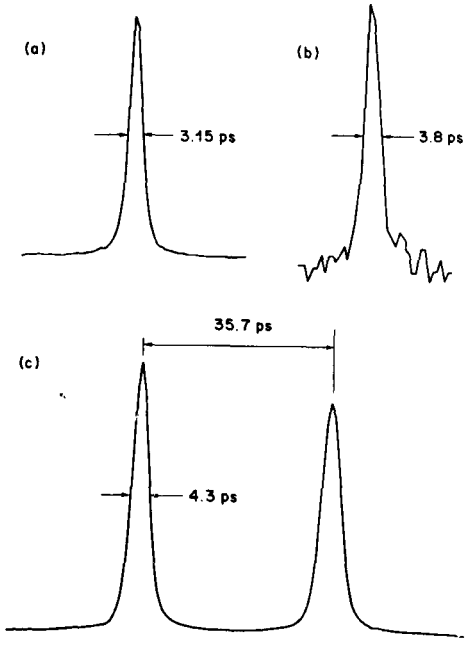

Figure 5. (a) The static resolution of the camera, (b) single shot dynamic resolution, (c) stacking of a sequence of 100 single shot events.

Conclusion

We showed that technology now enables the generation of optical pulses well into the femtosecond regime. We further demonstrated the operation of a subpicosecond jitter repetitively triggered streak camera. We expect that pulses on the femtosecond time scale will open the way to new applications in technology and new investigations in physics, chemistry and biology.

References

1. R. L. Fork, B. I. Greene, and C. V. Shank, Appl. Phys. Lett. 38, 671 (1981).
2. R. L. Fork, C. V. Shank, and R. Yen, Appl. Phys. Lett. 41, 273 (1982).
3. C. V. Shank, R. L. Fork, R. Yen, R. H. Stolen, and W. J. Tomlinson, Appl. Phys. Lett. 40, 761 (1982).
4. C. V. Shank, R. Yen, R. L. Fork, J. Orenstein, G. L. Baker, Phys. Rev. Lett. 49, 1660 (1982).
5. W. P. Su, J. R. Schrieffer, and A. J. Heeger, Phys. Rev. Lett. 42, 1698 (1979).

Picosecond electronic relaxations in amorphous semiconductors

Jan Tauc

Division of Engineering and Department of Physics, Brown University
Providence, Rhode Island 02912

Abstract

Using the pump and probe technique the relaxation processes of photogenerated carriers in amorphous tetrahedral semiconductors and chalcogenide glasses in the time domain from 0.5 ps to 1.4 ns have been studied. The results obtained on the following phenomena are reviewed: hot carrier thermalization in amorphous silicon; trapping of carriers in undoped a-Si:H; trapping of carriers in deep traps produced by doping; geminate recombination in $As_2S_{3-x}Se_x$ glasses.

Introduction

In recent years, amorphous semiconductors have been used in opto-eletronic applications, such as solar cells and picosecond detectors. The performance of these devices depends on the relaxation processes of photogenerated carriers, such as hot carrier thermalization, trapping and recombination. We have studed these processes in a broad time domain, from a fraction of a picosecond to hundreds of milliseconds in two representative groups of amorphous semiconductors, thin films of amorphous tetrahedral semiconductors and chalcogenide glasses. In this paper, we review some results obtained by the pump and probe technique in the range from 0.5 ps to 1.4 ns on undoped and doped a-Si:H and a-$As_2S_{3-x}Se_x$ glasses.

Experimental techniques

The experimental set-up is shown in Fig. 1. Subpicosecond pulses are produced by a passively mode-locked dye laser using the design by Ippen and Shank[1]. It produces linearly polarized transform-limited light pulses at $\hbar\omega_p$ = 2eV with pulse duration $t_p \approx$ 0.6 to 1 ps, energy 1 to 2 nJ and repetition rate 10^4 - 10^6 s^{-1}. The laser beam is divided into the pump (about 97% of the intensity) and probe. The pump is chopped by a mechanical chopper and focused on a spot on the sample of about 25 μm diameter. The probe passes through a polarization rotator so that its polarization relative to the pump can be changed. Then it is delayed by time τ by passing through a translation stage, focused on the same spot on the sample as the pump and finally on a detector (usually a Si photodiode). The signal from the detector is amplified by a lock-in amplifier and transformed into a multichannel analyser which integrates the responses over several scanning times of the translation stage.

The measured change of the absorption coefficient $\Delta\alpha$ is determined by the convolution of "response function" A(t) (defined as $\Delta\alpha$ produced by delta function excitation) with the pulse shapes. However, because the pump and probe have the same frequency, during the time that the pulses overlap there is an additional contribution due to an interference of the pulses, called "coherence artifact,"[2,3] which must be subtracted from the measured $\Delta\alpha$ before deconvoluting the data to find A(t). We found a method for doing this[3]. In the case of amorphous semiconductors $\Delta\alpha(t)$ measured with cross-polarized pump and probe is free of the coherent artifact.[3]

Electronic relaxations in amorphous semiconductors

A photon with energy $\hbar\omega_p$ absorbed in a semiconductor with an energy gap E_g produces a hot electron-hole pair if $\hbar\omega_p > E_g$. This process changes the absorption coefficient α of the medium. The number of initial states and the number of final states is reduced and consequently α is reduced. We will characterize this change by cross-section σ_o (>0) A more specific definition of σ_o is given in Ref. 4 with an estimate of its order in amorphous semiconductors (10^{-17} cm^2). The photogenerated carriers can absorb light by being excited into higher energy states and therefore their presence increases α; we will denote their absorption cross-section by σ_i (>0). If $\sigma_o > \sigma_i$ at the probe energy one observes photoinduced transmission (bleaching); if $\sigma_o < \sigma_i$ one observes photoinduced absorption. Bleaching is usually observed in crystalline semiconductors. The k-vector conservation law valid in a crystal makes free carrier absorption possible only if a

phonon takes part in the absorption process; the optical absorption cross-section is therefore usually smaller than σ_o. In an amorphous semiconductor, the k-vector conservation law does not apply, the free carrier absorption cross-section is usually larger than σ_o and induced absorption is observed.

The hot carriers quickly thermalize to the botton of the bands. In crystalline semiconductors, they stay there as free carriers for a long time until recombination occurs. In amorphous semiconductors (Fig. 2) they are trapped in shallow traps below the mobility edge. From there, they can go into deep traps and eventually recombine.

It is possible to follow these relaxation processes because σ_i depends on the state of the carrier at time t after excitation. We denote by σ_1 the absorption cross-sections of a hot carrier, σ_2 of a carrier in a shallow trap and σ_3 of a carrier in a deep trap. Since in the absence of k-vector conservation, the absorption by the probe depends on the density of final states which increases when one goes deeper into the band (Fig. 2), the absorption cross-sections σ_i tend to be smaller if the energy of the state is lower ($\sigma_1 > \sigma_2 > \sigma_3$). The cross-sections σ_1 and σ_2 are usually larger than σ_o; we shall see that in doped a-Si:H σ_3 is smaller than σ_o and induced transmission is observed.

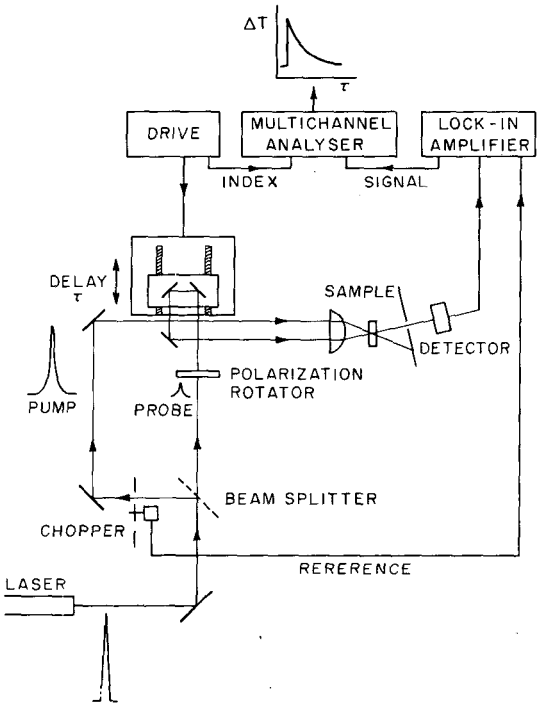

Fig. 1. The experimental set-up for studying picosecond relaxation of induced absorption.

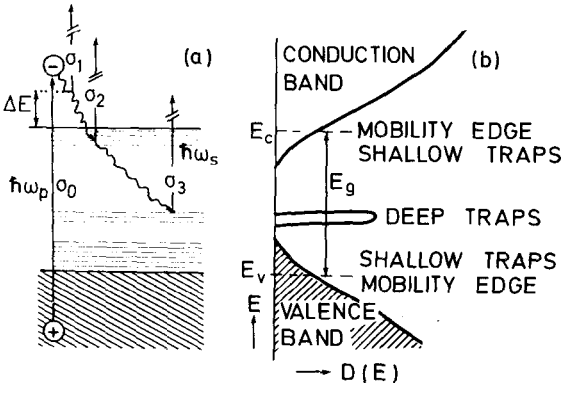

Fig. 2. Electronic relaxation processes in amorphous semiconductors:
(a) Generation of a hot electron-hole pair by absorption of a pump photon $\hbar\omega_p$ followed by their thermalization into shallow traps and then into deep traps. The processes are shown for the electron only, with cross-sections σ_1, σ_2 and σ_3 for the probe photon absorption. σ_{IR} is the cross-section for the midgap PA absorption (section V).

If the photon energy $\hbar\omega_p < E_g$ the photogenerated electron-hole pair is localized at one site. If the energy of this state is only slightly smaller than E_g thermal fluctuations may excite the carriers into the bands from which they will relax into traps. If the state is sufficiently deep the electron and hole do not move away from the site of excitation and eventually recombine with each other ("geminate recombination"). Geminate

recombination was observed in chalcogenide glasses and is discussed in the last section of this paper.

As we shall see on a few examples, the pump and probe technique enabled us to measure the rate of hot carrier thermalization and to determine the nature and the basic parameters of carrier transport into the traps. Another method for studying picosecond relaxations is photoconductivity ("PC"). Because the mobilities of trapped carriers are much smaller than the mobilities of carriers in the band, PC measures the time-evolution of the product effective mobility x concentration of carriers in the band while the probe and pump technique (photoinduced absorption "PA") measures the quantity $(\sigma_i - \sigma_0) \times n_i$ (n_i is the concentration of carriers in state i).

Hot carrier thermalization in amorphous Si

The responses measured[5] in a-Si, a-Si:H and a-Si:H:F in the first 10 ps after excitation are shown in Fig. 3. They were fitted using A(t) shown in Fig. 4 and interpreted as due to absorption of hot carriers that loose their excess energies during the thermalization time t_o and then sit in the states at the band edges producing little time dependent absorption $\Delta\alpha_s$. A justification for this interpretation is the dependence of the relative strength of the response at t = 0 defined as $(\Delta\alpha(o) - \Delta\alpha_s)/\Delta\alpha_s$ on hydrogen content C_H (Fig. 5). When C_H is larger, E_g is larger and the excess energy at t = 0 $E(0) = \hbar\omega_p - E_g$ is smaller; therefore σ_1 at t = 0 is expected to be smaller, as actually observed. The thermalization time t_o obtained from the fit was 0.7 ps for a-Si and 1.2 ps for a-Si:H.

Assuming that the excess energy E(0) is equally divided between the electron and the hole, we can calculate the average energy dissipation rate $R = \frac{1}{2} E(0)/t_o$ which was 0.5 eV/ps in a-Si and 0.1 eV/ps in a-Si:H. The value observed in the latter material can be obtained from hot electron-phonon interaction involving optical phonon deformation potential scattering with constant $D \simeq 5 \times 10^8$ eV cm^{-1}. The situation in a-Si is more complicated because here the electron-electron scattering is weaker than the electron-phonon scattering, and therefore an effective hot carrier temperature cannot be defined.[5] It is probable that the strong disorder in this material enhances the electron-phonon interaction.

Carrier trapping in undoped a-Si:H

As shown in Figs. 6 and 7 the saturation appearing in Fig. 3 is actually a slow decrease of $\Delta\alpha$ [6]. In these figures, the thermalization process is not resolved. Close to t = 0 some broadening occurs due to the finite pulse widths but the onset is instantaneous within our resolution. Then a decay follows which was faster in the sputtered (SP) sample reaching a saturation value in about 1 ns. In the high quality glow-discharge (GD) sample, the decay was slower and did not saturate in our time range. The interpretation of this observation is that carriers are trapped in deeper and deeper states where their absorption cross-section is smaller and smaller. Their trapping rate is higher if the concentration of traps is larger (the SP sample in Fig. 6 was of poorer quality and had more states in the gap than the GD sample). When all carriers are trapped, a new "saturation" occurs. Picosecond PC response in a-Si:H was recently reviewed by Johnson[7]. The curve shown in Fig. 8 was measured by the electronic correlation technique invented by Auston et al.[8] In this case, the true response is convoluted with the known response of another photoconductor which is fast. If we compare the rate of the PC decay (Fig. 8) with the PA decay (Fig. 6) in similar materials we see that the PC decay is much faster. As explained above, the PA response depends on the distribution of carriers in the states in the gap whose absorption cross-sections $\sigma_i(E)$ decrease when energy E moves deeper into the gap. The PC response depends on the mobility $\mu(E)$ of carriers in these states which decreases much more sharply with E than $\sigma_i(E)$ (the deeper states are more localized). The mobilities of trapped carriers are negligible and only carriers in the band contribute to PC. This explains why the PC decay becomes faster at low T (thermal excitation of trapped carriers is less probable) while the PA response is slower (a significant decrease of σ_i requires a deeper trap and at low T it takes a longer time for the carrier to reach it). For both PA and PC a higher defect concentration increases the decay rate (the decays are much faster in a-Si than in a-Si:H).

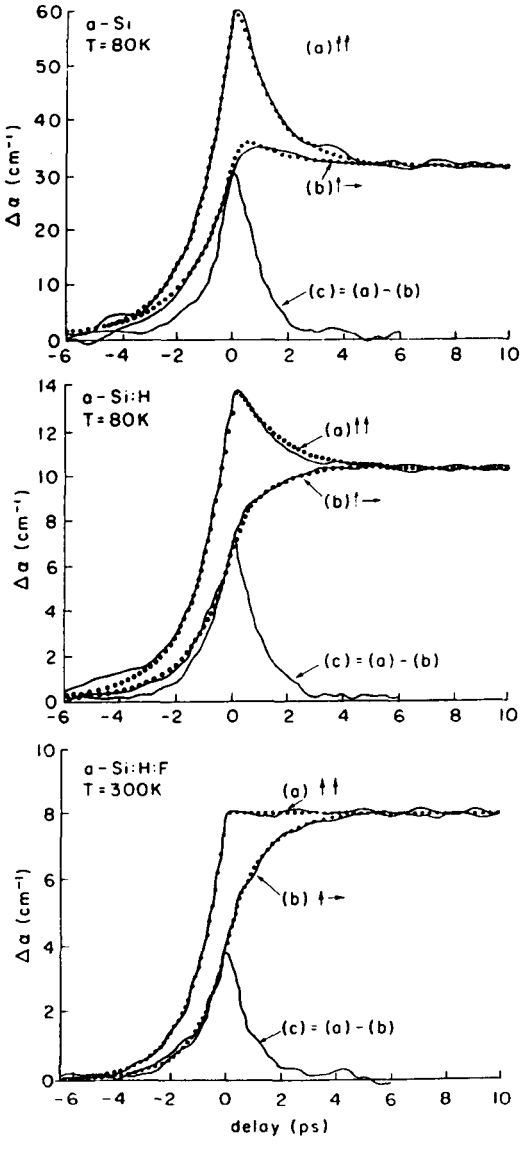

Fig. 3. Photoinduced absorption $\Delta\alpha(t)$ in a-Si, a-Si:H(C_H = 10 at %) and a-Si:H:F(C_H = 14 at %, C_F = 16 at %).

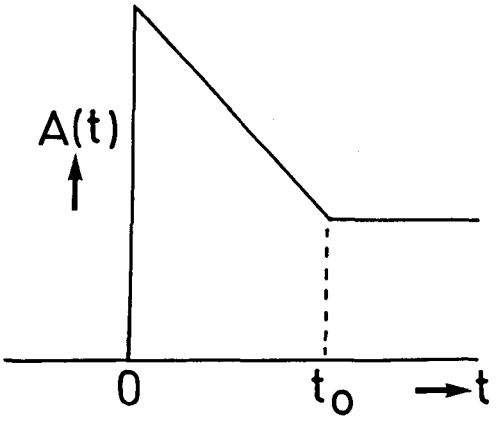

Fig. 4. Response function A(t) with which the data in Fig. 3 were fitted.

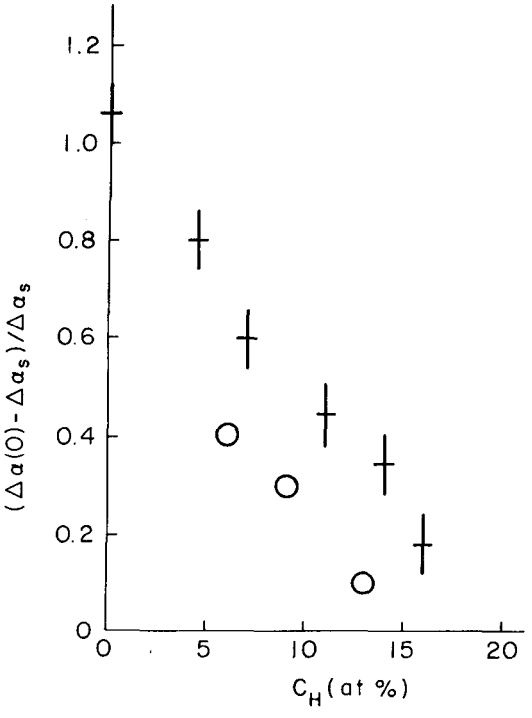

Fig. 5. The relative strengths of the induced absorption at t = 0 as a function of hydrogen content in a-Si:H (crosses) and a-Si:H:F (circles). C_F = 16 at %.

Carrier trapping in doped a-Si:H

As shown in Fig. 9, the decay rate is much faster in phosphorus doped a-Si:H than in undoped a-Si:H.[9] It is even more so in boron doped and compensated samples. Close to t = 0 one observes induced absorption which sharply decreases and eventually changes its sign becoming induced transmission. The decay is faster at higher temperature and higher P concentrations.

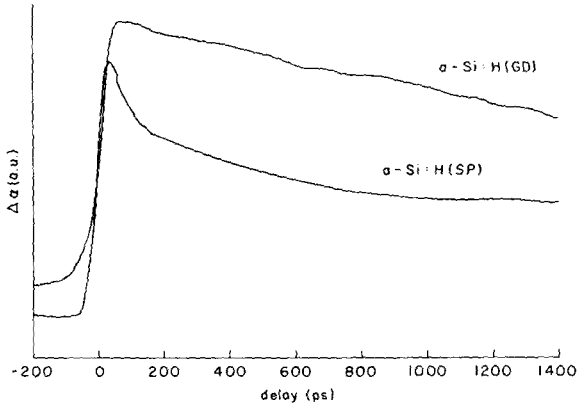

Fig. 6. Induced absorption decays in glow-discharge (GD) and sputtered (SP) a-Si:H at 300K.

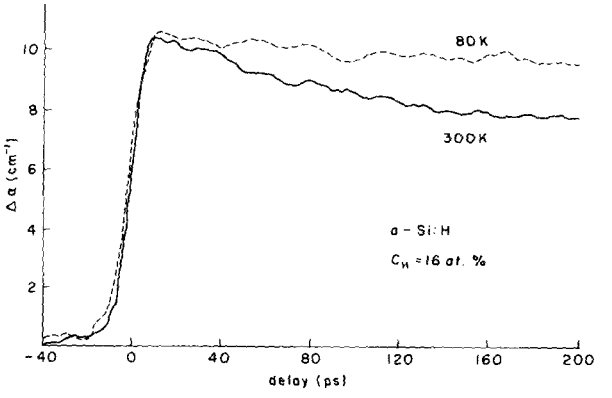

Fig. 7. Temperature dependence of the decay in a-Si:H (SP).

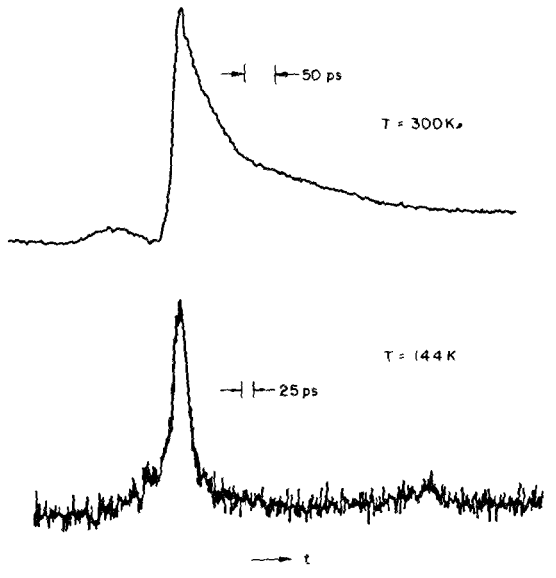

Fig. 8. Picosecond photoconductivity decays in a-Si:H, (from Johnson, Ref.7).

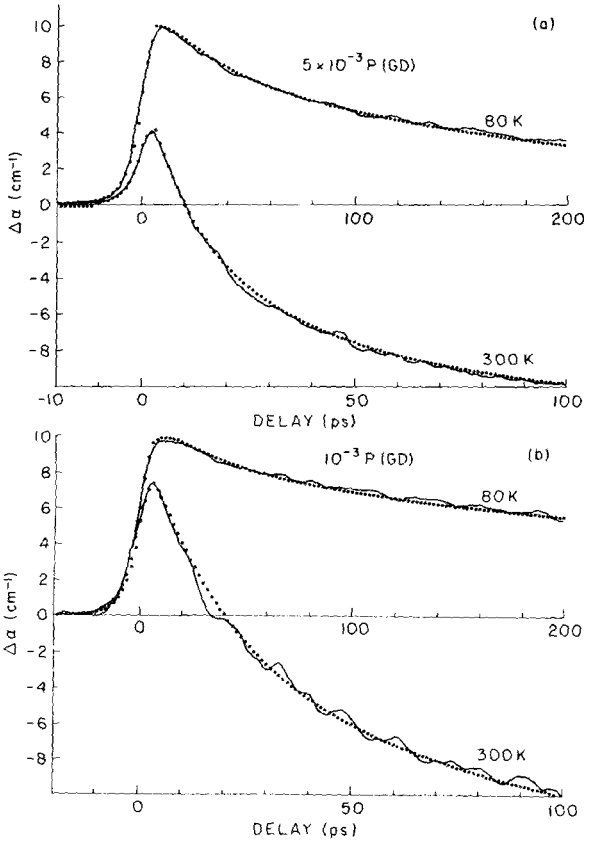

Fig. 9. Decays in P-doped glow discharge a-Si:H. Solid lines: experimental, dotted lines: calculated.

The enhancement of the decay rate by doping is explained by the presence of deep traps associated with doping a-Si:H with P and B. These elements, besides being n- or p-type dopants as in crystalline Si, introduce deep traps confined to a relatively narrow range of energy[10]. These deep trap have a very small absorption cross-section σ_3, apparently